An Evaluation of Shale Gas Potential in the Bowland Shale, UK using Sequential High Water Pressure Pyrolysis and Methane Adsorption*

P. Whitelaw[1,2], C. Uguna[1,2], L. Stevens[1], W. Meredith[1], C. E. Snape[1,2], C. Vane[2], V. Moss-Hayes[2], and A. D. Carr[3]

Search and Discovery Article #51450 (2017)**
Posted December 26, 2017

*Adapted from extended abstract based on oral presentation given at AAPG International Conference and Exhibition, London, England, October 15-18, 2017

[1]1University of Nottingham, Faculty of Engineering, Energy Technologies Building, Nottingham NG7 2TE, UK (Colin.Snape@nottingham.ac.uk)
[2]Centre for Environmental Geochemistry, British Geological Survey, Keyworth, Nottingham, UK
[3]Advanced Geochemical Systems Ltd., Burton-on-the-Wolds, Leicestershire, UK

Abstract

A recent study of the early Namurian Bowland Shale gas potential in northern England (UK), obtained using a 3D geological model and a statistical simulation, indicated 264 tcf gas in place (GIP, HIo = 475) (Andrews, 2013). This estimate assumes that dry gas (>80% methane, CH_4) is generated from kerogen in the range 1.1 to 1.9% Ro, even though the evidence from the USA is that maturities >1.4% Ro are required. In addition, the gas volume estimate assumes that the shale porosity and gas absorption in the Bowland Shale followed the trends published for USA analogues, e.g. Barnett Shale. The prediction of gas volumes generated assumes that gas is generated in a chemical reaction system containing only shale, whereas shales both prior and during gas generation contain water in pores and fractures and rock. Water plays important chemical and physical roles during both generation and absorption of petroleum. Using sequential (stepwise) pyrolysis involving repeated periods of heating (burial) with successively higher temperatures and time, followed by cooling (uplift) as in northern England, gas under non-hydrous conditions was generated containing <70% CH_4, whereas under high water pressures (550 bar and higher) > 90% CH_4 was generated. The maturity at which CH_4 contents >80% were generated appears to be >2% Ro. The GIP estimates calculated (using gas yield obtained for 800 bar sequential pyrolysis) at different maturities between 1.26-2.34% Ro assuming that all the generated gas remains within the shale. The GIP was highest at maturity of 1.26 to 2.03% Ro, but was a factor of 2-3 lower at Ro >2.0%. To provide precise estimates, the wetness of gas and maturity range for dry gas generation needs to be defined. For example, over a maturity range of 2.25-2.34% Ro and a gas dryness of 90%, the GIP estimate was ca. 22 tcf; 12 times lower than 264 tcf reported by Andrews (2013). Porosity determined using nitrogen, CO_2 and high pressure CH_4 adsorption isotherms conducted on shales both with and without moisture was used to provide information on the shale micropore structure. The mono-layer coverage from a Langmuir plot was calculated to be 1.8mg at 100°C and 4.2mg at 25°C of CH_4/g rock in wet samples, which are significantly lower (8-19 tcf) than that required to accommodate 264 tcf of gas. Andrews, I.J. 2013. The Carboniferous Bowland Shale: Geology and resource estimate. British Geological Survey for the Department of Energy and Climate Change, London, UK.

Introduction

Shale gas is often relatively dry (composed mainly of methane), implying that it is largely generated at high thermal maturities. Produced gas data from the Barnett Shale have shown a methane content of 80 % for the condensate-wet gas window and >90 % for the dry gas window (Jarvie et al. 2005, 2007), with produced gas from 131 Barnett Shale, and 101 Fayetteville Shale wells having methane contents in the ranges of 78-97 % and 92-98 %, respectively (Zumberge et al. 2012). In unconventional shale gas systems, it is generally accepted that gas generation results from the cracking of kerogen and petroleum (bitumen, and/or oil) retained in low porosity shales at relatively high maturities (Bernard et al. 2012; Hill et al. 2007; Jarvie et al. 2007). Jarvie (2012), based on studies on the producing wells for US shale gas plays, suggested that the best shale resource system should have a source rock maturity of > 1.4 % Ro. The gas window maturity of a source rock will depend on both kerogen type and thermal history; with predominantly type II kerogens expected to start generating gas at a lower maturity than type III or type II/III mixed source rocks due to their higher reactivity (Jarvie et al. 2005, 2007).

The successful exploitation of Barnett shale and other North American plays has led to a renewed interest in the geological evolution of the Carboniferous Bowland-(Hodder) shale, which is considered to be a potential major source of shale gas in the UK (Andrews 2013; Imber et al. 2014; Smith et al. 2010; Slowakiewicz et al. 2015). The study by Andrews (2013) estimated that the shale gas resources of the entire UK Carboniferous Bowland shale unit is significant, with the upper and lower units containing 164-447 and 658-1834 tcf (trillion cubic feet) of gas, respectively. However, this was based on adsorbed gas and free gas estimates for US shales and assumed that shale in the maturity range of 1.1-1.9 % Ro, had generated gas, contrary to the evidence for US shales (Jarvie et al., 2012).

Other laboratory techniques, such as micro-scale sealed-vessel (MSSV) and hydrous pyrolysis do measure gas yields, but the estimated shale gas yields are clearly going to be dependent on both the technique used and the maturity range over which it is assumed that the shale gas in place has been generated. MSSV uses glass tubes so that all volatiles are retained within the system (Mahlstedt and Horsfield, 2012; Yang et al., 2016). In contrast, hydrous pyrolysis that is also a closed system, oil generated can be expelled into the water phase so better mimicking actual expulsion of oil from source rocks (e.g Lewan, 1997). We have reported recently that high-pressure water pyrolysis in which there is no free space in the reactor vessel can be used to understand pressure effects with respect to both source rock maturation and hydrocarbon generation (Uguna et al. 2012, 2013, 2015, 2016). Clearly, pyrolysis methods will not give a unique value of shale gas potential because different maturity ranges are required to generate gas of varying dryness.

In this study, low pressure non-hydrous (5-20 bar) pyrolysis, which fairly closely resembles conditions in MSSV, and high pressure water pressure (180-800 bar) pyrolysis have been used to investigate the gas generation potential of a source rock (Rempstone 1 well, Widmerpool Trough, Figure 1) from the UK Carboniferous Bowland Shale unit. The goal is to understand not only the mechanism of dry gas formation containing over 80-90 % methane but to identify the maturity range over which this is generated. To achieve this, sequential pyrolysis was carried out where, after each experiment, the expelled oil and gas are recovered for analysis and maturities of 2.3-2.6 % Ro have been reached. This is designed to simulate oil and gas generation, during successive periods of burial (simulated by heating the rocks) and uplift (simulated by cooling the rocks) as experienced by the Carboniferous UK basins.

The other approach for assessing shale gas potential is to estimate the combined amount of adsorbed gas and free gas occupying the pore space in shales. The adsorbed gas can be estimated from high pressure methane adsorption isotherms and the free gas from a combination of nitrogen adsorption isotherms (BET) and Mercury Intrusion Porosimetry (MIP), the former measuring the micro and mesopore volumes with the latter determining the macropore volume. Such estimates may be low with the possibility of capillary condensation (Barsotti et al., 2016), especially for wet gas in organic rich shales is neglected. .US and Canadian shale porosities are 1-7 % of the total volume with free gas ranging from 20 to 270 scf/ton for US producing systems (Curtis 2002, Jarvie 2012, Ross and Bustin 2008). Micropore volumes are low but increase with maturity with ranges between 0.0006 (VR 1.15 %) to 0.012 cm^3/g (VR 2.5 %) being reported (Ross and Bustin 2008, Mastalerz et al. 2013). Methane adsorption capacities have been reported ranging from 0.26 (Eagle Ford) to 1.50 mg/g (Barnett) for US shales (Heller and Zoback 2014, measured at 40-50 bar) and between 1.00 to 4.08 mg/g for Qiongzhusi shale, China (Li et al. 2017, measured at 140 bar). Not surprisingly, these estimates are considerably lower than for isolated type II kerogen that had an adsorption capacity of 15 mg/g (Zhang et al. 2012). In this study, we make the first direct comparison between laboratory pyrolysis procedures and gas adsorption with pore volume measurements to estimate the maximum shale gas potential and demonstrate that, although ranges of values are obtained, these is consistency between the two approaches.

Geological Setting of Study Area

The Carboniferous, basal Namurian, Bowland shale formation was deposited in parts of the East Midlands, North Wales and Northern England in a series of subsiding grabens and half-grabens (Fraser and Gawthorpe, 1990; Leeder, 1982, 1988). The Formation consists of marine, hemipelagic shales deposited in the basins. In the Widmerpool Trough (Figure 1), the Remsptone-1 well is on the southern edge and the Bowland Shale is underlain by the Widmerpool Formation and other Visean shales. The shale rock investigated is from a borehole core (Rempstone-1 well) of Namurian (Arnbergian) age obtained at a depth of between 665-667 m. Cessation of rifting occurred across large parts of the UK during late Visean and was followed by a period of regional thermal subsidence. Shale deposition continued in the Widmerpool Trough, culminating with the siliclastic sandstones of the Millstone Grit Group. These sandstones represent the progradation of deltas across the Visean and early Namurian basins. The western, deepest part of the Widmerpool Trough was inverted and partially eroded by the Late Carboniferous inversion during the Variscan orogeny prior to deposition of Permo-Triassic rocks.

Experimental

Pyrolysis Prior to pyrolysis, the core was crushed into 2-5 mm chips that were thoroughly mixed to obtain a homogenous sample. Sequential pyrolysis tests have been carried out under non-hydrous (5-20 bar) and high pressure water pressure (800 bar) conditions in a 25 ml Hastalloy cylindrical pressure vessel rated to 1400 bar at 420 °C, connected to a pressure gauge and rupture disc rated to 950 bar. The experimental procedure used was described in detail by Uguna et al. (2012, 2015). The sequential experiments are depicted in Figure 2 and the conditions and quantities of rock used are listed in Table 1. The removal of the expelled oil and the gas after each maturity stage enables the maturity interval to be identified over which dry shale gas will be generated. At the higher temperatures of 380 and 420 °C used (Table 1 and Figure 2), the water is supercritical at 800 bar and will so behave as an organic solvent, which may lead to more oil expelled when compared to 350 °C (Uguna et al. 2015). It is acknowledged that supercritical water only exists in sedimentary geological basins with volcanic activity, but it was necessary to use such high temperatures to achieve high (dry gas window) maturities in reasonable times.

Gas samples were collected and analysed by gas chromatography. Vitrinite reflectance (VR) measurements were conducted on the initial (non-extracted) and pyrolysed rocks solvent extracted residues mounted in epoxy resin, using methods contained in ISO 7404-5:2009. Rock Eval pyrolysis and total organic carbon (TOC) analysis were conducted on the initial and pyrolysed non-extracted rocks from the sequential experiments.

Methane adsorption and pore volume determination Methane adsorption isotherms were obtained using a Particulates Systems (Micromeritics) High Pressure Volumetric Analyser I (HPVA) at 25, 60 and 100 °C up to pressures of 100 bar on both wet and dry shales. The crushed shale samples (2-5 mm) with moisture present (wet) or vacuum dried for 48 hrs at 70 °C (dry) were loaded into the sample cell. Skeletal density of the shale was calculated using helium pycnometry on the vacuum dried shale, with the assumption that helium penetrates all accessible porosity. Free space for analysis was calculated by taking the free space of the empty cell calculated from helium expansion minus the volume of the shale. Monolayer capacities were calculated using the dual site Langmuir equation to predict adsorption beyond the experimental range as it could not be reached through experimental means (Tang et al. 2016).

Micro and mesoporosity was analysed using nitrogen isotherms obtained with a Micrometrics ASAP 2420 Accelerated Surface Area and Porosimetry Analyser. These were obtained at -196 °C on shale samples (2-5 mm) in with both moisture present (wet) and vacuum dried for 48 hrs at 70 °C (dry). Adsorption and desorption isotherm between from relative pressure (p/po) of 0.01 to 0.99 was generated. Surface area of the shales was calculated using BET surface area equation from 0.05 to 0.20 relative pressure giving positive BET 'C' values.

Macro and mesopore volumes by MIP were measured with a Micrometrics Autopore IV Mercury Porosimeter. Shale samples (2-5 mm) were vacuum dried for 48 hrs at 70 °C, and placed within the pentrometer. The pressure applied was increased stepwise up to approximately 4137 bar and the volume of mercury entering the shale's pores and therefore pore volume penetrated by mercury at that pressure applied. The radii of the penetrated pores at a given pressure was calculated using the Washburn equation for slit shaped pores with a contact angle of 152.5° and a surface tension of 475.5 mN/m for mercury on shale (Wang et al. 2016).

Results and Discussion

Gas yields The methane and total hydrocarbon (C_1-C_5) gas yields for the sequential non-hydrous and 800 bar water pressure experiments are presented in Figure 3 and Figure 4. The gas dryness is correlated with vitrinite reflectance in Figure 5. The gas yields increased going from the first heating stage (350 °C, 24 h) to a maximum at 420 °C for 24 h (third stage), before decreasing at the fourth (420 °C, 48 h) and fifth (420 °C, 120 h) stages. The gas yields are considerably higher for the non-hydrous experiments between the second and fifth stages and the gas is wetter (dryness of only 0.69 and 0.66 after 4th and 5th stages compared to 0.80 and 0.90, respectively, with high pressure water). The difference arises because no expulsion of oil occurs in the non-hydrous experiments and it is the residual oil/bitumen that is responsible for producing much more gas that is considerably wetter. Therefore, only laboratory procedures where expulsion can occur, as in the high-pressure waster experiments, are capable of generating dry gas predominately from kerogen. The yields obtained from the final two stages in high-pressure water are a factor of 4 lower than those from non-hydrous pyrolysis (Figure 3 and Figure 4) at Ro greater than 2.

Dry gas formation (CH_4 >80 %) clearly occurs only after migration of the bulk of the oil and wet gas generated at lower maturities at >2 % Ro. Although it is believed that oil expulsion is highly restricted in unconventional petroleum systems due to the low porosity of shale rock, some does occur (Jarvie et al. 2007) who estimated that 60 % of oil generated by the Barnett Shale source rock was expelled, and only 40 % was retained for secondary cracking to gas. Therefore, dry pyrolysis methods (Rock-Eval, MSSV and gold bags) that do not expel oil will result in vast overestimations of shale gas GIP volumes as shown here for the non-hydrous pyrolysis.

Gas holding capacity of the shale (adsorbed and free methane) Obtaining high-pressure methane isotherms with condensed moisture and oil within the pores better represents geological conditions. The methane isotherms all displayed Type I behavior that can be fitted to the dual site Langmuir model (Figure 6) associated with micropore filling mechanism forming a monolayer. Table 2 lists the measured capacities at 100 bar and the derived extrapolated capacities at 250 bar and for a monolayer coverage for the shale sample obtained after the final stage from the high-pressure water experiments. The adsorption capacity increases with maturity (nearly three-fold for measurements on dry samples). Vacuum drying the sample to remove condensed moisture and oil increased the methane adsorption capacities roughly two fold due to competition for the same adsorption sites. As expected, with increasing temperature where 60-100 °C represents the temperature range for Rempstone shale having maturities of Ro > 2, Table 2 indicates that methane adsorption was reduced by 36 and 61 % at 60 and 100 °C compared to 25 °C. These reductions match other data published on the effects of temperature of CH_4 adsorption (Rexer et al., 2013). The measurements reported here were carried out at 50% relative humidity. The amount of adsorbed methane could be up to 30% lower at 100% relative humidity, comparing our results with those reported by Merkel et al. (2015).

Table 3 lists the BET surface areas, micro and total (micro plus meso) pore volumes from nitrogen adsorption isotherms, and the meso, macro and total pore volumes obtained from MIP for the initial shale and the samples obtained after stages 4 and 5 of the sequential high pressure water experiments. The results indicate that mesoporosity dominates the shale samples with the mesopore volumes accounting for over 70 % of the total for gas adsorption and over 90 % from MIP. The mesopore volumes from MIP are approximately 20-30 % higher than those from BET and this is typical for many samples where some deformation of the pore structure is considered likely at the high pressures used in MIP to intrude the mercury into narrower mesopores. This does not affect the macropore volumes as lower pressures are used compared to those required to force mercury into the smaller mesopores. Pore volume increases markedly at late maturity during the dry gas generating window consistent with the findings reported by Mastalerz et al. (2013) for New Albany shale. However, moisture and oil in the samples reduce the BET surface areas 80 % indicating these components are mainly in the micropores. Overall, for the matured shales, the decrease in mesopore volume is approximately 30 % with moisture present.

The porosity of Bowland shales in the Lancashire basin close to the gas window have porosities of 1% or below. This is considerably lower than the Rempstone sample, which has a much greater initial porosity due to its shallower depth and where the high-pressure water pyrolysis treatment is generated additional macroporosity.

Comparison of shale gas estimates from high pressure water pyrolysis and gas adsorption To compare the GIP estimates from our pyrolysis experiments and the adsorbed plus free gas measurements, two scenarios are used for the latter with the current day temperatures and hydrostatic pressures being assumed to be 60°C/150 bar and 100°C/300 bar covering many Bowland shales in the gas window. A porosity of 1% is used as typically found for a number of shales from the Lancashire basin. It is estimated on a volumetric basis, that the high pressure

pyrolysis gas yield of 63 scf/tonne across the whole gas window (stages 3-5) is less than the shale holding capacity (100-140 scf/tonne including 15-28 scf/tonne of free gas) means that the GIP is controlled by gas generation. The estimate by Andrews (2013) for Upper Bowland shales with a TOC of 4.5% is roughly 220-270 scf /tonne, ca. 4 times higher than the cumulative gas yield from high pressure water pyrolysis, is also clearly considerably higher than the estimated gas holding capacity meaning that the maximum GIP would be controlled by the holding capacity with expulsion having to occur to facilitate further gas generation with increasing maturity. The yield of gas from non-hydrous pyrolysis of 185 scf/tonne is also considerably higher than the total amount of adsorbed and free gas.

Gas in place estimates from pyrolysis To derive these estimates, the individual gas yields were converted from mg to volume using their different gas densities to obtained the total (C_1-C_5) gas volume (cubic feet), and the pyrolysed rock converted to volume assuming a shale density of 2.6 g/cm^3 (Andrews 2013). Our estimates have been calculated assuming the three different thermal maturity ranges from stages 3-5 for the high-pressure water experiments. The net volume (7.90 x 1011 m^3) for the Upper Bowland shale used by Andrew (2013) was apportioned with 57% of the volume lies between 1.1- 2.0%, 20% between Ro 2.0-2.3% and 23% > Ro. Further, the high-pressure water results have been converted to a TOC of 2%, close to the mean value estimated by Andrews (2013) for the Upper Bowland shale corresponding to a TOC of 2.0% and an initial HI similar to Rempstone.

Below Ro of 2.0, depending upon the level of retained oil, it is estimated that there will be either 16 tcf of wet gas (stage 3 for Rempstone, Figure 4) or 8 tcf of dry gas if retained oil levels are very low in Bowland shales at Ro>1.25. The latter is the amount of gas that was generated across this maturity range in high-pressure water pyrolysis for a core from the Lancashire basin that only contained 1% retained oil. At Ro > 2.0% when only dry gas is produced, the GIP increases by 21 tcf if no expulsion occurs giving at total of either 23 tcf dry gas or up to 38 tcf of wetter gas. This makes the estimated GIP volume to be 7-10 times lower compared to 264 tcf reported by Andrews (2013). Although much less is currently known about the Lower Bowland shale, it is estimated to be 4 times as large in terms of volume than Upper Bowland, the lower TOC will be roughly offset by the higher overall maturity of the shale (Andrews, 2013). These estimates are the maximum that can be obtained as migration of some gas at relatively high maturities may be possible, especially during extensive uplift. Given that UK gas consumption is currently 2.7 tcf p.a. and, assuming a 10% recovery, the entire Bowland shale represents less than 10 years supply.

Conclusions

Unlike dry/anhydrous pyrolysis, high-pressure water pressure pyrolysis is capable of generating dry gas (> 80 % as found for many shales) sequentially after expelled oil and wet gas is removed. Thus, it is the only laboratory procedure that can be used to model shale gas generation. For the Rempstone shale, dry gas (>80% methane) is generated at > 2.0 % Ro and at lower maturities wet gas is obtained, the cumulative volume being 85 scf/tonne and the wet gas reduces if more of the remaining oil is expelled at lower maturity. Through adsorption and free gas in the pores, low porosity shales with TOCs close to 4.5% as for the matured Rempstone samples can store up to ca. 140 scf/tonne at 100 oC at 300 bar, suggesting that generation rather than holding capacity is the limiting factor for GIP for Bowland shale.

The implications to the gas shale prospectivity are that the thermal maturity range (1.1-1.9% Ro) suggested by Andrews (2013) for extensive gas generation is too low for dry gas generation. Indeed, wet gas will only be found with shale oil at Ro of 1.1. Although Bowland shale with high maturity needs to be targeted for exploration for dry gas, this will only provide the UK with gas for no more than 10 years based on

current consumption. However, it is important to note that our estimate is based on only one shale, and more source rocks from the Bowland Shale unit need to be investigated to obtain a much-improved reliable and representative estimate of the shale gas potential in northern England.

Acknowledgements

The authors thank Statoil, Woodside Energy and the National Environmental Research Council for supporting the development of the high-pressure water pyrolysis technique and British Geological Survey, Centre for Environmental Geochemistry for a research fellowship for Dr. Clement Uguna.

References Cited

Andrews, I.J., 2013, The Carboniferous Bowland Shale: Geology and resource estimate: British Geological Survey for Department of Energy and Climate Change, London, UK.

Barsotti, E., S.P. Tan, S. Saraji, M. Piri, and S-H. Chen, 2016, A review on capillary condensation in nanoporous media: Implications for hydrocarbon recovery from tight reservoirs: Fuel, v. 184, p. 344-361.

Bernard, S., R. Wirth, A. Schreiber, Hans-M. Schulz, and B. Horsfield, B., 2012, Formation of nanoporous pyrobitumen residues during maturation of the Barnett shale (Fort Worth basin): International Journal of Coal Geology v. 103, p. 3-11.

Curtis. J.B., 2002, Fractured Shale Gas systems: AAPG Bulletin, v. 86. p. 1921-1938

Fraser, A.J., and R.L. Gawthorpe, 1990, Tectono-stratigraphic development and hydrocarbon habitat of the Carboniferous in northern England: in R.F.P. Hardman and J. Brooks, (Eds.), Tectonic Events Responsible for Britain's Oil and Gas Reserves, Geological Society Special Publication No 55, p. 49-86.

Heller, R., and M. Zoback, 2014, Adsorption of methane and carbon dioxide on gas shale and pure mineral samples: Journal of Unconventional Oil and Gas Resources, v. 8, p. 14-24.

Hill, R.J., D.M. Jarvie, J. Zumberge, M. Henery, and R.M. Pollastro, 2007, Oil and gas geochemistry and petroleum systems of the Fort Worth Basin: AAPG Bulletin, v. 91, p. 445-473.

Imber, J., H. Armstrong, S. Clancy, S. Daniels, L. Herringshaw, K. McCaffrey, J. Rodrigues, J. Trabucho-Alexandre, and C. Warren, 2014, Natural fractures in a United Kingdom shale reservoir analog, Cleveland basin northeast England: AAPG Bulletin, v. 98, p. 2411-2437.

International Organisation for Standardisation (ISO), 2009, Methods for the petrographic analysis of coals-Part 5: Method of determining microscopically the reflectance of vitrinite: ISO 7404-5:2009, ISO, Geneva.

Jarvie, D.M., 2012, Shale resource systems for oil and gas: Part 1 - Shale-gas resource systems: in J.A. Breyer, (Ed.), shale reservoirs– Giant resources for the 21st century: AAPG Memoir 97, p. 69-87.

Jarvie, D.M., R.J. Hill, T.E. Ruble, and R.M. Pollastro, 2007, Unconventional shale-gas systems: The Mississippian Barnett Shale of north-central Texas as one model for thermogenic shale-gas assessment: AAPG Bulletin, v. 91, p. 475-499.

Jarvie, D.M., R.J. Hill, and R.M. Pollastro, 2005, Assessment of the gas potential and yields from shales: The Barnett Shale model: in B.J. Cardott, (Ed.), Unconventional energy resources in the Southern Mid-Continent, 2004 symposium: Oklahoma Geological Survey Circular 110, p. 37-50.

Leeder, M.R., 1982, Upper Palaeozoic basins of the British Isles-Caledonide inheritance versus Hercynian plate margin process: Journal of the Geological Society of London, v. 139, p. 479-491.

Leeder, M.R., 1988, Recent developments in Carboniferous geology: a critical review with implications for the British Isles and N.W. Europe: Proceedings of the Geologists Association, v. 99, p. 73-100.

Lewan, M.D., 1997, Experiments on the role of water in petroleum formation: Geochimica et Cosmochimica Acta, v. 61, p. 3691-3723.

Li, A., W. Ding, X. Zhou, X. Cao, M. Zhang, F. Fu, and E. Chen, 2017, Investigation of the Methane Adsorption Characteristics of Marine Shale: A Case Study of Lower Cambrian Qiongzhusi Shale in Eastern Yunnan Province, South China: Energy & Fuels, v. 31, p. 2625-2635.

Mahlstedt, M., and B. Horsfield, 2012, Metagenetic methane generation in gas shales I. Screening protocols using immature samples: Marine and Petroleum Geology, v. 31, p. 27-42.

Mastalerz, M., A. Schimmelmann, A. Drobniak, and Y. Chen, 2013, Porosity of Devonian and Mississippian New Albany Shale across a maturation gradient: Insights from organic petrology, gas adsorption, and mercury intrusion: AAPG Bulletin, v. 97, p. 1621-1643.

Rexer, T.F., M.J. Benham, A.C. Aplin, and K.M. Thomas, 2013, Methane adsorption on shale under simulated geological temperature and pressure conditions: Energy & Fuels, v. 27, p. 3099- 3109.

Ross, D.J.K., and M. Bustin, 2008, The importance of shale composition and pore structure upon gas storage potential of shale gas reservoirs: Martine and Petroleum Geology, v. 26, p. 916-927.

Slowakiewicz, M., M.E. Tucker, C.H. Vane, R. Harding, A. Collins, and R.D. Pancost, 2015, Shale gas potential of the mid Carboniferous Bowland Hodder unit in the Cleveland basin (Yorkshire) central Britain: Journal of Petroleum Geology, v. 38, p. 59-76.

Smith, N., P. Turner, and G. Williams, 2010, UK data and analysis for shale gas prospectivity: in S.C. Pickering and B.A. Vining, (Eds.), Petroleum Geology: From mature basins to new frontiers. Petroleum Geology Conference Series 7, p. 1087-1098.

Tang, X., N. Ripepi, N.P. Stadie, L. Yu, and M. Hall, 2016, A dual-site Langmuir equation for accurate estimation of high pressure deep shale gas resources: Fuel, v. 185, p. 10-17.

Uguna, C.N., A.D. Carr, C.E. Snape, W. Meredith, and M. Castro-Díaz, 2012, A laboratory pyrolysis study to investigate the effect of water pressure on hydrocarbon generation and maturation of coals in geological basins: Organic Geochemistry, v. 52, p. 103-113.

Uguna, C.N., M.H. Azri, C.E. Snape, W. Meredith, and A.D. Carr, 2013, A hydrous pyrolysis study to ascertain how gas yields and the extent of maturation for partially matured source rock and bitumen in isolation compared to their whole source rock: Journal of Analytical and Applied Pyrolysis, v. 103, p. 268-277.

Uguna, C.N., A.D. Carr, C.E. Snape, and W. Meredith, 2015, High pressure water pyrolysis of coal to evaluate the role of pressure on hydrocarbon generation and source rock maturation at high maturities under geological conditions: Organic Geochemistry, v. 78, p. 44-51.

Uguna, C.N., A.D. Carr, C.E. Snape, W. Meredith, I.C. Scotchman, A. Murray, and C.H. Vane, 2016, Impact of high water pressure on oil generation and maturation in Kimmeridge Clay and Monterey source rocks: Implication for petroleum retention and gas generation in shale gas systems: Journal of Marine and Petroleum Geology, v. 73, p. 72-85.

Wang, S., F. Javadpour, and Q. Feng, 2016, Confinement Correction to mercury intrusion capillary pressure of shale nanopores: Scientific Reports, v. 6, p. 20160.

Yang, S., B. Horsfield, N. Mahlstedt, M. Stephenson, and S. Könitzer, 2016, On the primary and secondary petroleum generating characteristics of the Bowland Shale, northern England: J. Geol. Soc., v. 173, p. 292-305.

Zhang, T., G.S. Ellis, S.C. Ruppel, K. Milliken, and R. Yang, 2012, Effect of organic-matter type and thermal maturity on methane adsorption in shale-gas systems: Organic Geochemistry, v. 47, p. 120-131.

Zumberge, J., K. Ferworn, and S. Brown, 2012, Isotopic reversal (‘rollover’) in shale gases produced from the Mississippian Barnet and Fayetteville formations: Marine and Petroleum Geology, v. 31, p. 43-52.

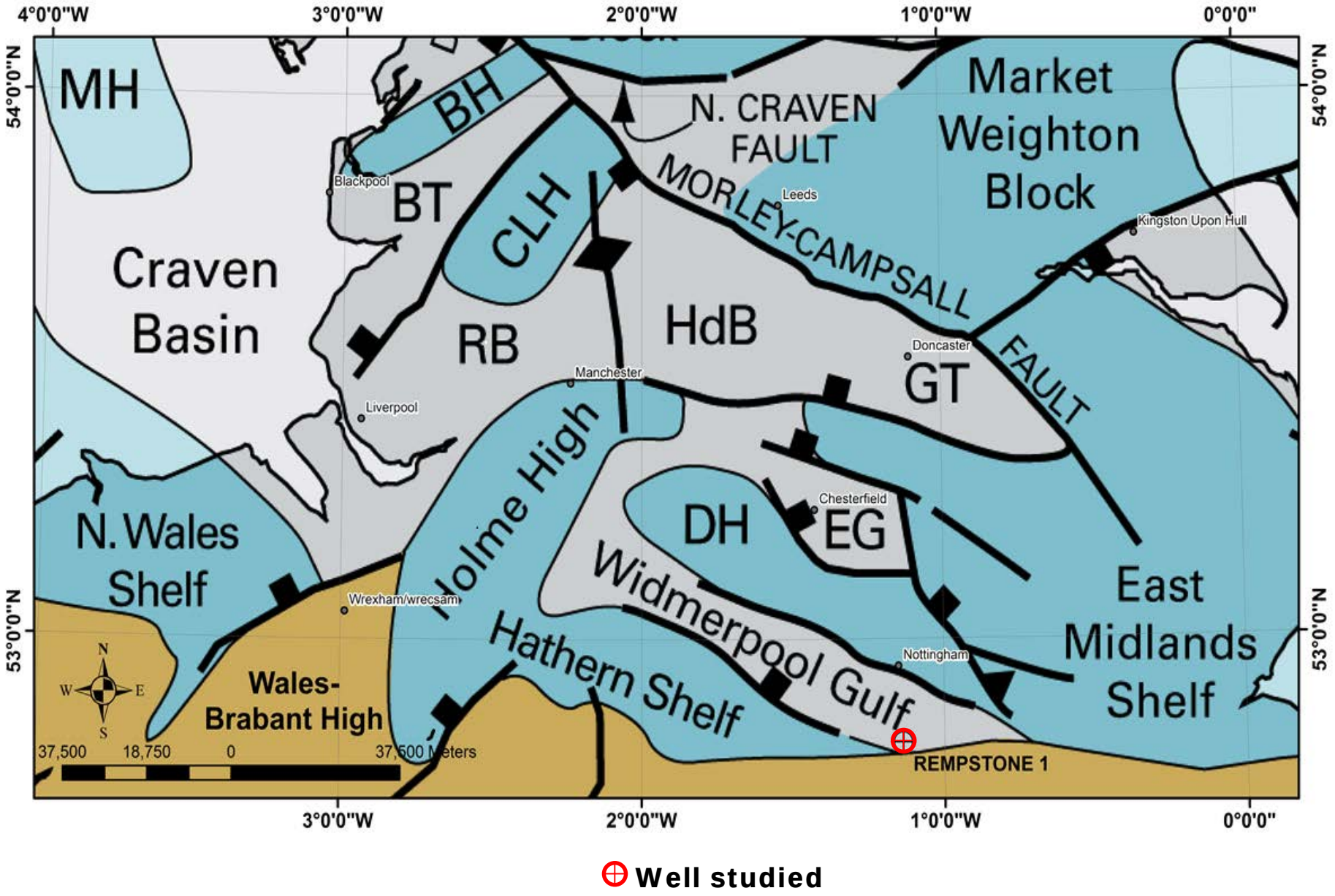

Figure 1. Map showing study area and location of Rempstone-1well (modified after Fraser and Gawthorpe 1990).

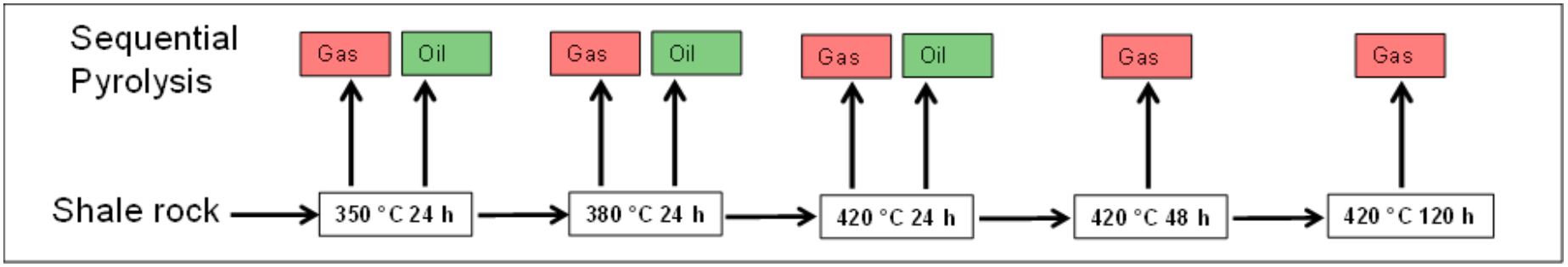

Figure 2. Schematic diagram showing the temperatures and times used for the sequential pyrolysis experiments.

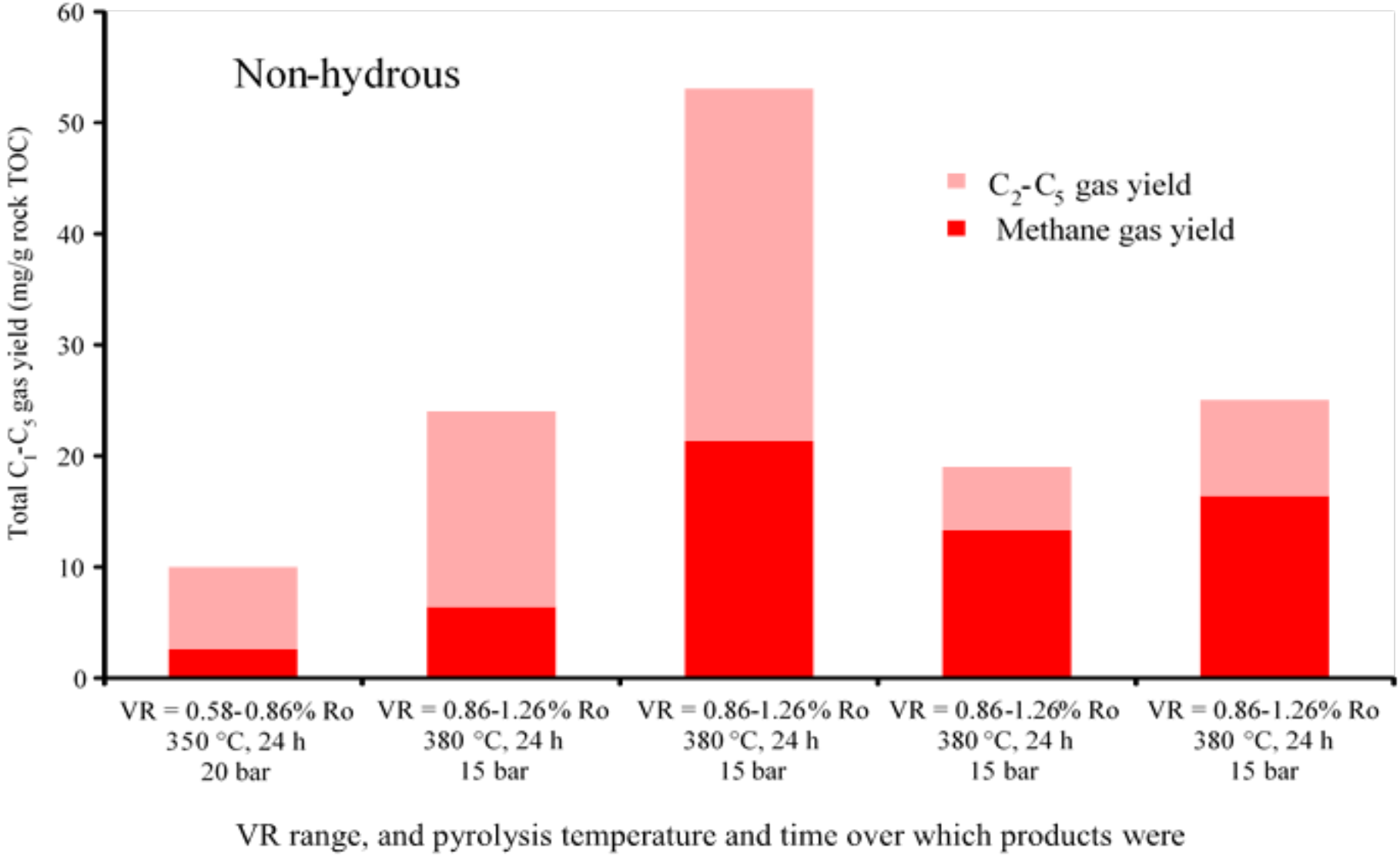

Figure 3. Total hydrocarbon (C_1-C_5), C_2-C_5 and methane yields (mg/g TOC of initial rock TOC before each pyrolysis step) for non-hydrous sequential pyrolysis.

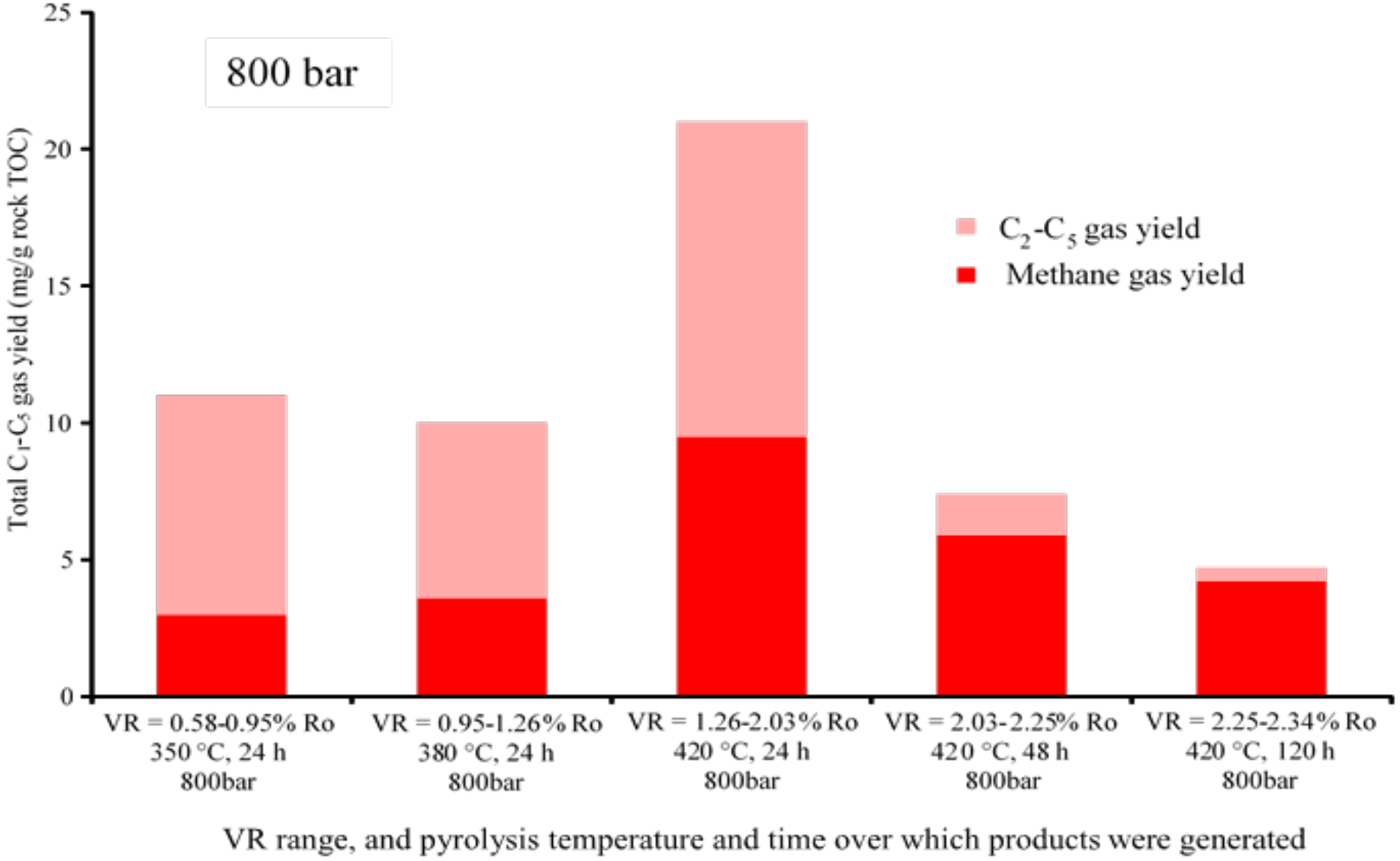

Figure 4. Total hydrocarbon (C_1-C_5), C_2-C_5 and methane yields (mg/g TOC of initial rock TOC before each pyrolysis step) for 800 bar sequential pyrolysis.

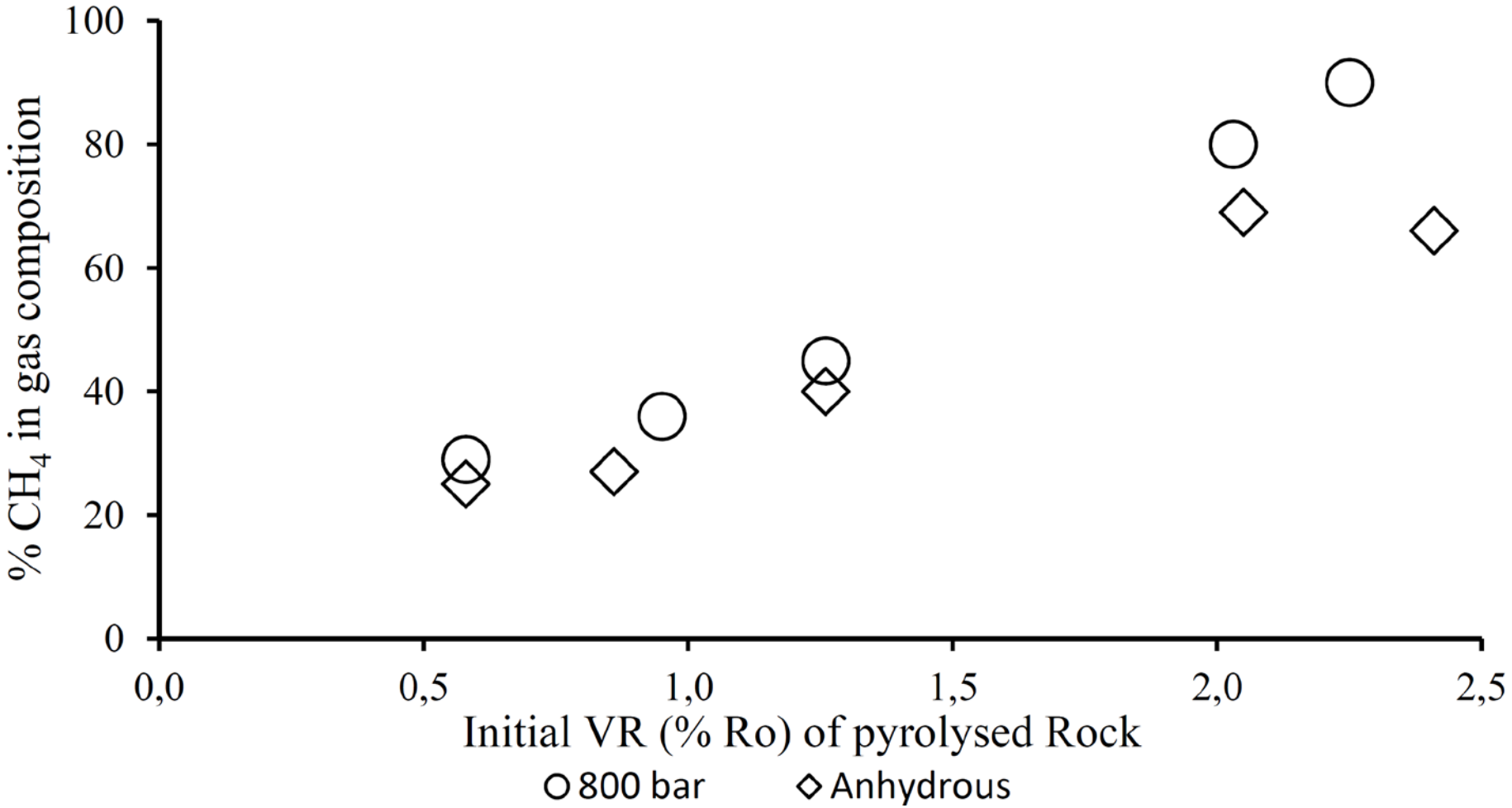

Figure 5. Gas dryness and final VR of the pyrolysed rocks.

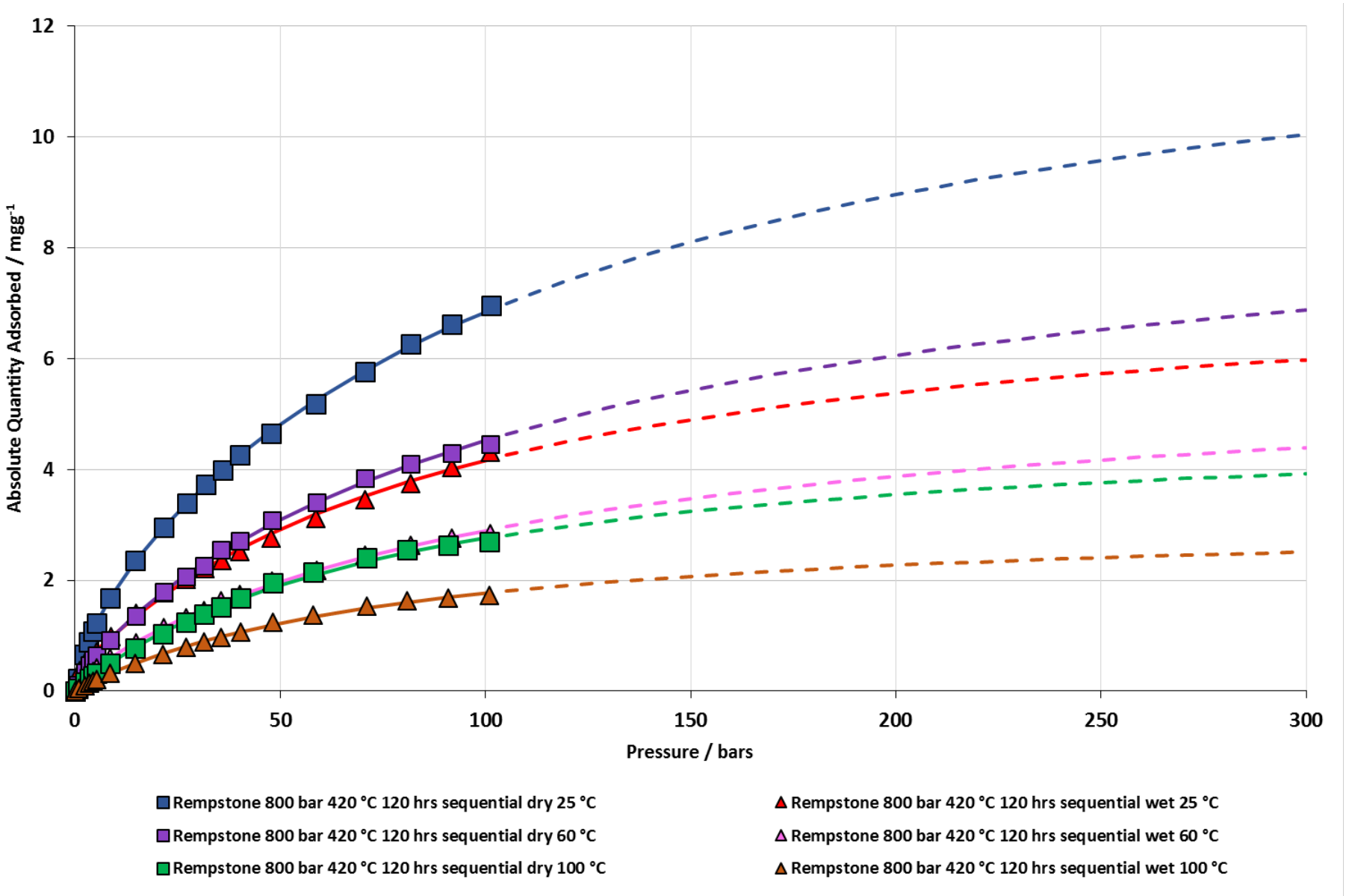

Figure 6. High-pressure methane adsorption isotherms fitted to the dual site Langmuir model for wet and dry samples for matured shale samples from stages 4 and 5 of the sequential high-pressure water experiments.

Experiment	Rock mass (g)	Temperature, time	Water pressure	Final pressure (bar)
Non-hydrous				
1st heating	19.0	350 °C, 24 h	none	20
2nd heating	14.5	380 °C, 24 h	none	15
3rd heating	10.9	420 °C, 24 h	none	10
4th heating	7.8	420 °C, 48 h	none	5
5th heating	4.1	420 °C, 120 h	none	5
800 bar water pressure				
1st heating	19.0	350 °C, 24 h	800 bar	850
2nd heating	14.9	380 °C, 24 h	800 bar	825
3rd heating	11.1	420 °C, 24 h	800 bar	805
4th heating	7.4	420 °C, 48 h	800 bar	805
5th heating	3.8	420 °C, 120 h	800 bar	800

Table 1. Experimental conditions and the amounts of rock used for the sequential pyrolysis.

Sample	100 bar (mg g^{-1})	250 bar (mg g^{-1})	Qm (mg g^{-1})
Wet 25 °C	4.3	5.7	7.7
Dry 25 °C	7.0	9.6	13.5
Wet 60 °C	2.9	4.2	6.1
Dry 60 °C	4.5	6.5	9.5
Wet 100 °C	1.3	2.4	3.2
Dry 100 °C	2.7	3.8	5.0

Table 2. Mono-layer CH_4 adsorption capacities for the Rempstone shale after sequential high pressure water pyrolysis (800 bar, 420 °C for 120 hrs, stage 5).

Sample	BET SA / m^2g^{-1}		V_{meso} / cm^3g^{-1}		V_{micro} / cm^3g^{-1}	
	Wet	Dry	Wet	Dry	Wet	Dry
Rempstone initial	1.6	16.9	0.004	0.016	<0.001	0.007
Stage 1	6.2	8.9	0.014	0.016	0.001	0.003
Stage 2	9.0	23.4	0.016	0.026	0.002	0.007
Stage 3	11.1	37.8	0.018	0.027	0.003	0.013
Stage 4	10.5	46.7	0.017	0.029	0.003	0.016
Stage 5	9.6	54.7	0.016	0.029	0.002	0.019

Table 3. BET and MIP pore volume measurements for the initial Rempstone shale and after stages 4 and 5 or the sequential high pressure water pyrolysis.